

QCD effective charge from the three-gluon vertex of the background-field method

D. Binosi,¹ D. Ibañez,² and J. Papavassiliou²

¹*European Centre for Theoretical Studies in Nuclear Physics
and Related Areas (ECT*) and Fondazione Bruno Kessler,*

Villa Tambosi, Strada delle Tabarelle 286, I-38123 Villazzano (TN) Italy

²*Department of Theoretical Physics and IFIC, University of Valencia E-46100,
Valencia, Spain*

Abstract

In this article we study in detail the prospects of determining the infrared finite QCD effective charge from a special kinematic limit of the vertex function corresponding to three background gluons. This particular Green's function satisfies a QED-like Ward identity, relating it to the gluon propagator, with no reference to the ghost sector. Consequently, its longitudinal form factors may be expressed entirely in terms of the corresponding gluon wave function, whose inverse is proportional to the effective charge. After reviewing certain important theoretical properties, we consider a typical lattice quantity involving this vertex, and derive its exact dependence on the various form factors, for arbitrary momenta. We then focus on the particular momentum configuration that eliminates any dependence on the (unknown) transverse form factors, projecting out only the desired quantity. A preliminary numerical analysis indicates that the effective charge is relatively insensitive to the numerical uncertainties that may afflict future simulations of the aforementioned lattice quantity. The numerical difficulties associated with a parallel determination of the dynamical gluon mass are briefly discussed.

PACS numbers: 12.38.Aw, 12.38.Lg, 14.70.Dj

I. INTRODUCTION

The ongoing quest for a deeper understanding of the nonperturbative features of the basic Green's functions of QCD has been benefited considerably by the constructive interaction between lattice simulations and the Schwinger-Dyson equations (SDEs). One of the central issues in this search is the systematic study of how the effects of dynamical mass generation manifest themselves in the nonperturbative structure of the propagators of the fundamental fields (quarks, gluons, and ghosts). In particular, the concept of a momentum-dependent gluon mass [1] has received renewed attention, because it provides a natural explanation for the infrared finiteness of the gluon propagator, $\Delta(q^2)$, and ghost dressing function, $F(q^2)$, observed in large-volume lattice simulations carried out in the Landau gauge, both in $SU(2)$ [2] and in $SU(3)$ [3].

Especially interesting in this context is the definition and properties of the QCD effective charge, as well as its interplay with the gluon mass. In fact, as has been explained in detail in a series of works [4–6], if the finiteness of the aforementioned Green's functions is to be attributed to the dynamical generation of a gluon mass [*i.e.*, $\Delta^{-1}(0) = m^2(0)$], then the corresponding effective charge, when properly defined, saturates also at a finite, nonvanishing value [1, 5]. Within this picture, the so-called “freezing” of the charge is a consequence of the presence of the gluon mass in the corresponding logarithms, which are cured from the perturbative Landau pole, are well-defined for all physical momenta, and acquire a finite value at $q^2 = 0$. It is important to emphasize that this characteristic property of the QCD coupling, which endows the theory with an infrared fixed point, has been advocated by a large number of very distinct theoretical and phenomenological approaches, see [1, 5, 7–14] and references therein.

A self-consistent framework for the study of the effective charge is provided by the fusion of the pinch technique (PT) [1, 15–19] with the background field method (BFM) [20], known in the literature as the “PT-BFM” scheme [21–23]. The natural starting point in this context is the PT gluon propagator, $\widehat{\Delta}(q^2)$, which is known to coincide with the two-point function of two background gluons. Note that $\widehat{\Delta}(q^2)$ and $\Delta(q^2)$, as well as their individual kinematic components introduced below, are related by powerful identities [24, 25] [see, *e.g.*, Eq. (2.9)], involving an auxiliary two-point function, which, in the deep infrared, practically coincides with the ghost dressing function [26, 27].

In the presence of a dynamically generated mass, the (Euclidean) $\widehat{\Delta}(q^2)$ assumes the form $\widehat{\Delta}^{-1}(q^2) = q^2 \widehat{J}(q^2) + \widehat{m}^2(q^2)$, where the first term corresponds to the “kinetic term”, or “wave function” contribution, while the second denotes the momentum-dependent mass [28]. Then, the (infrared finite) effective charge $\overline{\alpha}(q^2)$ may be defined as $\overline{\alpha}(q^2) = \alpha_s(\mu^2) \widehat{J}^{-1}(q^2, \mu^2)$, where μ is the renormalization (subtraction) point chosen, within an appropriate renormalization scheme [28]. By virtue of the QED-like Ward identities (WIs) satisfied in the PT-BFM framework, this latter quantity is formally renormalization group (RG)-invariant (μ -independent). Note that the freezing property of this $\overline{\alpha}(q^2)$ hinges crucially on the fact that the infrared finiteness of $\widehat{\Delta}(q^2)$ has been accounted for by the inclusion of the $\widehat{m}^2(q^2)$ in the above decomposition; instead, the alternative definition in terms of the gluon dressing function $\widehat{Z}(q^2) = q^2 \widehat{\Delta}(q^2)$, namely $\overline{\alpha}(q^2) = \alpha_s(\mu^2) \widehat{Z}(q^2, \mu^2)$, gives rise to a RG-invariant effective charge that vanishes trivially at the origin [5].

Evidently, in order to proceed further with the determination of the physical effective charge, one needs information on the behavior of $\widehat{J}(q^2)$. To be sure, $\widehat{J}(q^2)$ could be obtained from Eq. (2.13) if its conventional counterpart, $J(q^2)$, were known; however, unlike $F(q^2)$, this latter quantity may not be directly extracted from existing lattice simulations. Indeed, the lattice determines the full propagator $\Delta(q^2)$, but offers no direct information on the momentum dependence of the individual components.

Similarly, within the nonperturbative PT-BFM framework, both $\widehat{J}(q^2)$ and $\widehat{m}^2(q^2)$ satisfy independent (but coupled) non-linear integral equations, which are obtained from the SDE of the $\widehat{\Delta}(q^2)$ following a well-defined procedure, developed in a series of recent works [29, 30]. These two equations may, in principle, determine the complete dynamics of these two quantities. In practice, however, one is considerably limited by the fact that the main ingredients entering in them are the (largely unexplored) fully dressed three- and four-gluon vertices, for arbitrary values of their momenta, and, as a result, only approximate solutions may be obtained.

It would be clearly desirable, therefore, to determine $\widehat{J}(q^2)$ from an approach that is *ab-initio* exact, in the sense that it does not involve any field-theoretic approximations. To that end, in this article we explore the possibility of extracting this important quantity from a possible lattice simulation of the PT-BFM three-gluon vertex [15, 31], to be denoted by $\widehat{\Gamma}$, defined as the one-particle irreducible part of the correlation function involving three background gluons (the prospects for a lattice nonperturbative formulation of the BFM have

been recently revitalized due to the results of [32, 33]).

The fundamental reason why this vertex can furnish clean information on $\widehat{J}(q^2)$ is the Abelian WI that it satisfies [15]. Specifically, to all orders in perturbation theory this WI involves only the difference of $\widehat{\Delta}^{-1}(q^2) = q^2\widehat{J}(q^2)$, defined at the appropriate momenta; this is to be contrasted with the usual Slavnov-Taylor identity (STI) satisfied by the conventional three-gluon vertex [34], which involves, in addition, contributions from the ghost-sector of the theory, and especially from the so-called ghost-gluon kernel [35].

Of course, to properly account for mass generation, $\widehat{\Gamma}$ must be supplemented by a special nonperturbative vertex, denoted by \widehat{V} , which contains the necessary poles to enforce gauge invariance in the presence of a gluon mass [29]. This particular vertex is completely longitudinally coupled, and its divergence furnishes precisely the missing mass terms that convert $q^2\widehat{J}(q^2)$ into a massive $\widehat{\Delta}^{-1}(q^2)$, thus maintaining the form of the original WI intact. However, when the full vertex $\widehat{\Gamma} + \widehat{V}$ is contracted by three polarization tensors, as happens typically in lattice calculations in the Landau gauge [36], any reference on the (completely longitudinal) \widehat{V} disappears [29], and only the dependence on the nonperturbative \widehat{J} , defined at different momenta scales, survives. Then, a special kinematic limit, frequently employed in the lattice studies of three-point functions [36], converts the lattice quantity of interest into a function of a single variable, given simply by the first derivative of $q^2\widehat{J}(q^2)$. Finally, a straightforward integration of the lattice result over the relevant momentum interval furnishes $\widehat{J}(q^2)$, and consequently $\overline{\alpha}(q^2)$; this constitutes the central result of the present work.

It is clear that the usefulness of the aforementioned exact result must be assessed within the context of a realistic lattice simulation, taking into account, to some extent, the practical limitations associated with such an endeavor. In particular, it is important to provide a rough estimate of the errors that the various numerical uncertainties may introduce to the effective charge and, subsequently, the gluon mass. A simple modeling of these effects reveals that the predictions obtained for the effective charge are rather robust, and that the induced deviations do not alter significantly its theoretically expected behavior. Instead, with the exception of the deep infrared, the extraction of the gluon mass is afflicted by important qualitative discrepancies.

The article is organized as follows. In Sec. II we define the basic quantities appearing in this problem, and summarize some important relations, characteristic to the PT-BFM framework. In Sec. III we introduce the RG-invariant definition of the QCD effective charge

and of the gluon mass; in particular, we put forth an interesting analogy between this latter RG-invariant mass and the standard constituent quark mass. In Sec. IV we present the relevant three-gluon vertex, together with its basic properties. Particular attention is paid to the linear (ghost-free) WI satisfied by this vertex, which allows for the complete determination of its longitudinal form factors in terms of the gluon propagator, with no reference to ghost Green's functions. Sec. V contains the main results of the paper. First, we briefly review the general prospects of simulating PT-BFM Green's functions on the lattice. Then, assuming that such a simulation can be actually carried out for the vertex, we show how the effective charge and gluon mass can be directly reconstructed from the data obtained in a commonly used kinematical limit. In addition, we carry out a detailed numerical study on how the unavoidable numerical errors of a possible simulation propagate to the relevant physical quantities. Our analysis shows that, while a faithful approximation of the effective charge can be generally obtained, the reconstruction of the gluon running mass is much more subtle, displaying large fluctuations due to the inevitable distortion of delicate numerical cancellations. Finally, our conclusions are presented in Sec. VI.

II. GENERAL CONSIDERATIONS

The full gluon propagator $i\Delta_{\mu\nu}^{ab}(q) = \delta^{ab}\Delta_{\mu\nu}(q)$ in the Landau gauge is defined as

$$\Delta_{\mu\nu}(q) = -iP_{\mu\nu}(q)\Delta(q^2), \quad (2.1)$$

where

$$P_{\mu\nu}(q) = g_{\mu\nu} - \frac{q_\mu q_\nu}{q^2} \quad (2.2)$$

is the usual transverse projector, and the scalar cofactor $\Delta(q^2)$ is related to the (all-order) gluon self-energy $\Pi_{\mu\nu}(q) = P_{\mu\nu}(q)\Pi(q^2)$ through

$$\Delta^{-1}(q^2) = q^2 + i\Pi(q^2). \quad (2.3)$$

It is advantageous to introduce the *inverse* of the gluon dressing function, $J(q^2)$, defined as [35]

$$\Delta^{-1}(q^2) = q^2 J(q^2). \quad (2.4)$$

At tree-level, $J(q^2) = 1$. Perturbatively, at one-loop, it is given by

$$J(q^2) = 1 + \frac{13C_A g^2}{96\pi^2} \ln\left(\frac{q^2}{\mu^2}\right), \quad (2.5)$$

where C_A denotes the Casimir eigenvalue of the adjoint representation [$C_A = N$ for $SU(N)$], and the renormalization has been carried out in the momentum-subtraction (MOM) scheme. Evidently, $J^{-1}(q^2)$ displays a Landau pole at $q^2 = \mu^2 \exp(-96\pi^2/13C_A g^2)$.

The generation of a dynamical gluon mass leads to the infrared finiteness of the gluon propagator, to be denoted by $\Delta_m(q^2)$. In particular, in Minkowski space one has

$$\Delta_m^{-1}(q^2) = q^2 J_m(q^2) - m^2(q^2), \quad (2.6)$$

with $m^2(0) \neq 0$. The subscript “ m ” in J_m indicates that the resulting expressions are regulated by the presence of $m^2(q^2)$. Specifically, after gluon mass generation, the $J_m(q^2)$ may be *qualitatively* described by

$$J_m(q^2) = 1 + \frac{13C_A g^2}{96\pi^2} \ln \left(\frac{q^2 + \rho m^2(q^2)}{\mu^2} \right), \quad (2.7)$$

with g^2 , the constant ρ , and $m^2(q^2)$ such that $J_m(q^2) > 0$ for all values of q^2 , thus avoiding completely the appearance of a Landau pole.

The detailed dynamics that govern $J_m(q^2)$ and $m^2(q^2)$ are determined by two coupled integral equations, obtained from the SDE of the gluon propagator. Specifically, after a nontrivial reorganization of terms, one obtains an inhomogeneous equation for $J_m(q^2)$, and a homogeneous one for $m^2(q^2)$, of the general form [29, 30]

$$\begin{aligned} J_m(q^2)[1 + G(q^2)] &= 1 + \mu^\epsilon \int \frac{d^d k}{(2\pi)^d} \mathcal{K}_1(k, q, m^2, \Delta_m), \\ m^2(q^2)[1 + G(q^2)] &= \mu^\epsilon \int \frac{d^d k}{(2\pi)^d} \mathcal{K}_2(k, q, m^2, \Delta_m), \end{aligned} \quad (2.8)$$

where $d = 4 - \epsilon$ is the space-time dimension and μ the 't Hooft mass. Note that the corresponding kernels are such that, as $q \rightarrow 0$, $\mathcal{K}_{1,2}(k, q, m^2, \Delta_m) \neq 0$; in fact, in Euclidean space, the solution of these equations furnishes $J_m(q^2) > 0$ and $m^2(q^2) > 0$, as expected on physical grounds.

The appearance of the factor $[1 + G(q^2)]$ on the lhs of Eq. (2.8) stems from the fact that the corresponding equations are not derived from the standard SDE for the gluon propagator, but rather from its PT-BFM version; the advantages of this particular approach have been explained in detail in a series of articles [21–23]. In the PT-BFM formalism the natural separation of the gluonic field into a “quantum” (Q) and a “background” (B) gives rise to an extended set of Feynman rules, and leads to an increase in the type of possible

Green's functions that one may consider. In the case of the gluonic two-point function, in addition to the conventional QQ gluon propagator, Δ , two additional quantities appear: the QB propagator, $\tilde{\Delta}$, mixing one quantum gluon with one background gluon, and the BB propagator, $\hat{\Delta}$, with two background gluon legs. It turns out that these three propagators are related by the all-order identities [24, 25]

$$\Delta(q^2) = [1 + G(q^2)]\tilde{\Delta}(q^2) = [1 + G(q^2)]^2\hat{\Delta}(q^2), \quad (2.9)$$

usually referred to as Background-Quantum identities (BQIs).

The function $G(q^2)$ is defined as the $g_{\mu\nu}$ component of the special two-point function

$$\begin{aligned} \Lambda_{\mu\nu}(q) &= -ig^2\mu^\epsilon C_A \int \frac{d^d k}{(2\pi)^d} \Delta_\mu^\sigma(k) D(q-k) H_{\nu\sigma}(-q, q-k, k) \\ &= g_{\mu\nu} G(q^2) + \frac{q_\mu q_\nu}{q^2} L(q^2), \end{aligned} \quad (2.10)$$

where $D^{ab}(q^2) = \delta^{ab} D(q^2)$ is the ghost propagator, and $H_{\nu\sigma}$ is the gluon-ghost kernel [37, 38]. Perturbatively, at one-loop, we have (Landau gauge, MOM scheme)

$$1 + G(q^2) = 1 + \frac{9 C_A g^2}{2 \cdot 96\pi^2} \ln\left(\frac{q^2}{\mu^2}\right). \quad (2.11)$$

Just as the usual quantum gluon propagator, the BB propagator $\hat{\Delta}$ is also infrared finite, and must be parametrized in complete analogy with Eq. (2.6), namely

$$\hat{\Delta}_m^{-1}(q^2) = q^2 \hat{J}_m(q^2) - \hat{m}^2(q^2), \quad (2.12)$$

and an exactly analogous formula holds for $\tilde{\Delta}$ (not used here). Then, one can establish that the BQIs hold individually for the kinetic and mass terms, *i.e.*,

$$\hat{J}_m(q^2) = [1 + G(q^2)]^2 J_m(q^2), \quad (2.13)$$

$$\hat{m}^2(q^2) = [1 + G(q^2)]^2 m^2(q^2) \quad (2.14)$$

Use of Eq. (2.13), together with Eq. (2.11) and Eq. (2.5), furnishes the one-loop perturbative expression for $\hat{J}(q^2)$, namely

$$\hat{J}(q^2) = 1 + bg^2 \ln\left(\frac{q^2}{\mu^2}\right), \quad (2.15)$$

where $b = 11C_A/48\pi^2$ is the first coefficient of the QCD β -function. Evidently, as is well-known [20], the propagator $\hat{\Delta}(q^2)$ absorbs all the RG logarithms, exactly as happens in QED with the photon self-energy.

III. EFFECTIVE CHARGE AND RG-INVARIANT GLUON MASS

Let us next recall that, due to the Abelian WIs satisfied by the PT-BFM Green's functions, the renormalization constants of the gauge-coupling and of $\widehat{\Delta}(q^2)$, defined as

$$\begin{aligned} g(\mu^2) &= Z_g^{-1}(\mu^2)g_0, \\ \widehat{\Delta}(q^2, \mu^2) &= \widehat{Z}_A^{-1}(\mu^2)\widehat{\Delta}_0(q^2), \end{aligned} \quad (3.1)$$

where the “0” subscript indicates bare quantities, satisfy the QED-like relation

$$Z_g = \widehat{Z}_A^{-1/2}. \quad (3.2)$$

As a result, the product

$$\bar{d}_0(q^2) \equiv g_0^2 \widehat{\Delta}_0(q^2) = g^2 \widehat{\Delta}(q^2) \equiv \bar{d}(q^2), \quad (3.3)$$

forms a RG invariant (μ -independent) quantity. As has been explained in the recent literature [28], $\bar{d}(q^2)$ may be cast in the form

$$\bar{d}(q^2) = \frac{\bar{g}^2(q^2)}{q^2 + \bar{m}^2(q^2)}, \quad (3.4)$$

with

$$\bar{g}^2(q^2) = g^2 \widehat{J}_m^{-1}(q^2), \quad (3.5)$$

and

$$\bar{m}^2(q^2) = \widehat{m}^2(q^2) \widehat{J}_m^{-1}(q^2). \quad (3.6)$$

Note that the two quantities defined above are individually RG invariant. The usual effective charge, $\bar{\alpha}(q^2)$, is obtained from Eq. (3.5) simply as $\bar{\alpha}(q^2) \equiv \bar{g}^2(q^2)/4\pi$. At one-loop,

$$\bar{g}^2(q^2) = \frac{g^2}{1 + bg^2 \ln(q^2/\mu^2)} = \frac{1}{b \ln(q^2/\Lambda^2)}. \quad (3.7)$$

where Λ denotes an RG invariant mass scale of a few hundred MeV.

It is interesting to observe the analogy between the RG invariant mass defined in Eq. (3.6) and the corresponding constituent quark mass, familiar from a plethora of studies on chiral symmetry breaking. Specifically, the quark propagator is usually cast in the form

$$\begin{aligned} S^{-1}(p) &= A(p^2)\not{p} - B(p^2)\mathbb{I} \\ &= A(p^2)[\not{p} - \mathcal{M}(p^2)\mathbb{I}], \end{aligned} \quad (3.8)$$

where \mathbb{I} is the identity matrix, and the term $A^{-1}(p^2)$ is often referred to in the literature as the “quark wave function”. Note that, the quark acquires a dynamical mass (signaling the breaking of chiral symmetry) provided that $B(p^2)$ is different from zero, and that the constituent quark mass, $\mathcal{M}(p^2) = B(p^2)/A(p^2)$, is RG invariant. Then, it is natural to propose an analogy between the gluon and quark propagators; clearly, $\widehat{J}_m(q^2)$ corresponds to $A(p^2)$, while \widehat{m}^2 plays exactly the role of $B(p^2)$. Then, the division by $\widehat{J}_m(q^2)$ and $A(p^2)$ gives rise, in both cases, to RG invariant masses, suggesting a close correspondence between $\overline{m}^2(q^2)$ and $\mathcal{M}(p^2)$.

Next, using the BQIs (2.13) and (2.14) to relate the components of $\widehat{\Delta}_m(q^2)$ to the corresponding ones of $\Delta_m(q^2)$, we get

$$\widehat{m}^2(q^2)\widehat{J}_m^{-1}(q^2) = m^2(q^2)J_m^{-1}(q^2), \quad (3.9)$$

which finally furnishes a set of relations equivalent to (3.5) and (3.6),

$$\overline{g}^2(q^2) = g^2[1 + G(q^2)]^{-2}J_m^{-1}(q^2), \quad (3.10)$$

$$\overline{m}^2(q^2) = \widehat{m}^2(q^2)[1 + G(q^2)]^{-2}J_m^{-1}(q^2). \quad (3.11)$$

The basic Eqs. (3.5) and (3.6), or alternatively Eqs. (3.10) and (3.11), express the fundamental quantities $\overline{g}^2(q^2)$ and $\overline{m}^2(q^2)$ in terms of $\widehat{J}_m(q^2)$, or $J_m(q^2)$ and $G(q^2)$, respectively. It is therefore important to review the state-of-the-art in the determination of these quantities, both in the continuum as well as on the lattice.

To that end, let us first focus on the quantities $J_m(q^2)$ and $G(q^2)$, defined in the context of the conventional covariant gauges; in fact, we will specialize the discussion in the Landau gauge, where lattice simulations are usually performed.

Let us say from the outset that lattice simulations of the gluon propagator $\Delta_m(q^2)$ cannot furnish $J_m(q^2)$ without any additional input, for the simple reason that they provide the entire combination of $J_m(q^2)$ and $m^2(q^2)$, as appears in Eq. (2.6), but not the individual components comprising it. The SDEs, on the other hand, when appropriately reorganized, give rise to two coupled integral equations, one for $J_m(q^2)$ and one for $m^2(q^2)$, as shown schematically in Eq. (2.8). In principle these two equations should furnish the exact behavior of $J_m(q^2)$ and $m^2(q^2)$; in practice, one is limited by the fact that the closed form of the kernels \mathcal{K}_1 and \mathcal{K}_2 are only approximately known. In fact, \mathcal{K}_2 is better known than \mathcal{K}_1 , mainly because the only unknown quantity that enters in \mathcal{K}_2 is the full three-gluon vertex $\Gamma_{\alpha\mu\nu}$,

whereas in \mathcal{K}_1 appears, in addition, the full four-gluon vertex. Even though neither of these two vertices is known, the STIs that the three-gluon vertex satisfies [see Eq. (4.5)] furnish nontrivial information on the structure of its longitudinal components, thus providing certain field-theoretically motivated approximations for \mathcal{K}_2 ; on the contrary, no such construction exists for the four-gluon vertex, which remains practically unexplored.

The situation described above has motivated the advent of an approach which combines the information from both the lattice and the SDEs. In particular, instead of solving the system of Eq. (2.8), only the mass equation (involving the better known \mathcal{K}_2) is solved, using as input in it the lattice data for $\Delta_m(q^2)$. Then, once a solution for $m^2(q^2)$ has been obtained, one can use Eq. (2.6) to extract the approximate form of $J_m(q^2)$.

Regarding the function $G(q^2)$, notice that, quite remarkably, in the Landau gauge it coincides with the so-called Kugo-Ojima function [26, 27]. In addition, there is a deep connection between the form factors $G(q^2)$ and $L(q^2)$ and the ghost dressing function

$$F(q^2) = q^2 D(q^2), \quad (3.12)$$

expressed through the identity [26, 27]

$$1 + G(q^2) + L(q^2) = F^{-1}(q^2). \quad (3.13)$$

Since in $d = 4$ it is known that $L(q^2) \ll G(q^2)$ over the entire momentum range [27], one finally arrives at the result

$$1 + G(q^2) \approx F^{-1}(q^2), \quad (3.14)$$

which becomes an exact relation at $q^2 = 0$, since in this case $L(0) = 0$.

From the above discussion it is clear that one cannot obtain direct information on $J_m(q^2)$ from the gluonic two point sector. Turning to the three-point functions, one might think that, given that $J_m(q^2)$ enters into the longitudinal components of the conventional three-gluon vertex, as first demonstrated by Ball and Chiu [35], a judicious combination of them could project it out. However, the problem in this case is the ‘‘contamination’’ from the various form-factors comprising $H_{\mu\nu}$, which enter nontrivially in the various expressions.

It turns out that the PT-BFM three-gluon vertex lends itself for this type of analysis. Given that it satisfies QED-like WIs instead of STIs, there is no ghost sector contributions: the longitudinal form factors can be expressed in terms of the \widehat{J}_m only. To be sure, the transverse form factors enter in general, and are unknown. But, as we will see in Sec. V, there

is a simple kinematic limit, studied usually in the lattice simulations of the (conventional) vertex, which eliminates completely the transverse components, and projects out solely the first derivative of $q^2 \widehat{J}_m(q^2)$. It is therefore clear that a possible lattice extraction of $\widehat{J}_m(q^2)$ would provide an immediate determination of $\overline{g}^2(q^2)$ from Eq. (3.5).

On the other hand, regarding the prospects of extracting the RG invariant gluon mass from Eq. (3.6) or (3.11), one may envisage two basic scenarios [again assuming independent knowledge of $\widehat{J}_m(q^2)$]:

- (i) $\widehat{\Delta}_m(q^2)$ has been simulated on the lattice. Then, it is direct to extract $\widehat{m}^2(q^2)$ from Eq. (2.12), since (Euclidean space)

$$\widehat{m}^2(q^2) = \widehat{\Delta}_m^{-1}(q^2) - q^2 \widehat{J}_m(q^2), \quad (3.15)$$

or, using Eq. (3.6),

$$\overline{m}^2(q^2) = \widehat{\Delta}_m^{-1}(q^2) \widehat{J}_m^{-1}(q^2) - q^2. \quad (3.16)$$

- (ii) $\widehat{\Delta}_m(q^2)$ has not been simulated on the lattice. Then, to proceed further, one must necessarily employ the BQIs; this is rather feasible, because, as mentioned earlier, the function $G(q^2)$ has been simulated on the lattice. Specifically, one may use the conventional $\Delta_m(q^2)$ obtained from the lattice together with $G(q^2)$ to build $\widehat{\Delta}_m(q^2)$ by means of the BQI. Then one may return to the previous case (i), and substitute it into Eqs. (3.15) and (3.16).

This general discussion motivates a systematic study of the PT-BFM three-gluon vertex. To that end, in the next section we will present a brief reminder on the structure and general properties of the B^3 vertex, while in Sec. V after summarizing the current prospects of simulating nonperturbative PT-BFM Green's functions on the lattice, we will consider how $\widehat{J}(q^2)$ may be extracted from a possible lattice simulation of this vertex.

IV. THE PT-BFM THREE-GLUON VERTEX

The gauge-invariant three-gluon vertex $\widehat{\Gamma}_{\alpha\mu\nu}$ has been first considered in [15], where its one-loop construction was carried out by means of the PT, and its basic WI was derived (see also [19]). It was further studied in [31], with particular emphasis on the special relations between gluonic, fermionic, and scalar loop contributions, and has been revisited very recently in [39], using string-inspired techniques.

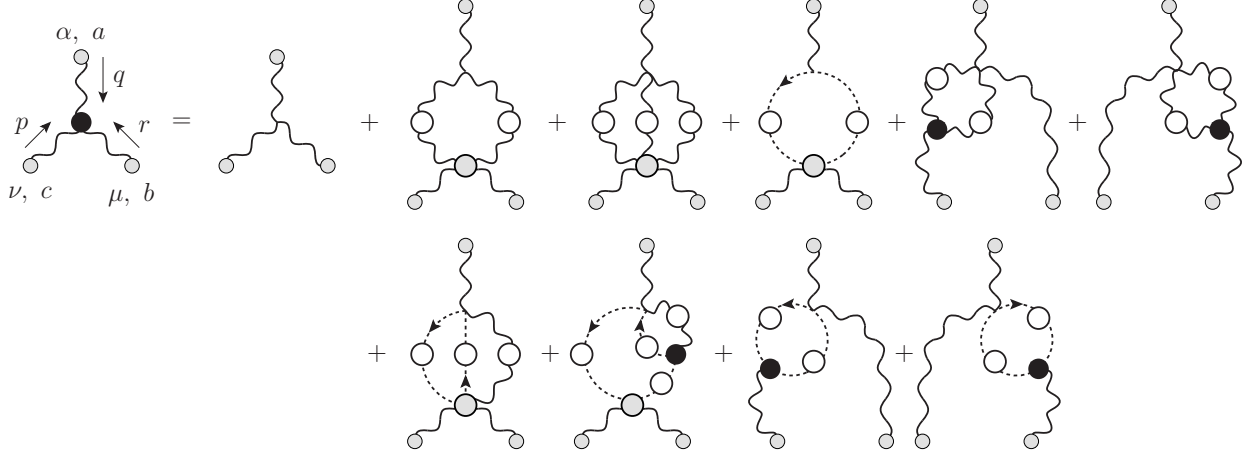


FIG. 1: The one-particle irreducible B^3 vertex and the SDE it satisfies. Background legs are indicated by the small circle at their end; black circles correspond to 1PI Green's functions, white circles represent connected functions, while gray circles indicate SDE kernels. The corresponding symmetry factors may be found in [23].

A. General properties

The equivalence between PT (or the “generalized PT”) and BFM allows for a concise field-theoretic definition of this vertex, as vacuum expectation value of the time-ordered product of three background gluons. In particular, denoting the full connected three-point function by (momentum space)

$$\widehat{\mathcal{G}}_{\alpha\mu\nu}^{abc}(q, r, p) = \frac{\langle 0 | T[\widehat{A}_\alpha^a(q)\widehat{A}_\mu^b(r)\widehat{A}_\nu^c(p)] | 0 \rangle}{\langle 0|0 \rangle}, \quad (4.1)$$

one defines

$$\widehat{\mathcal{G}}_{\alpha\mu\nu}^{abc}(q, r, p) = \widehat{\Delta}_{\alpha\alpha'}^{aa'}(q)\widehat{\Delta}_{\mu\mu'}^{bb'}(r)\widehat{\Delta}_{\nu\nu'}^{cc'}(p)\widehat{\Gamma}_{\alpha'\mu'\nu'}^{a'b'c'}(q, r, p), \quad (4.2)$$

where $\widehat{\Gamma}_{\alpha\mu\nu}(q, r, p)$ is the amputated three-point function.

Exactly as happens with the conventional three-gluon vertex $\Gamma_{\alpha\mu\nu}$, the $\widehat{\Gamma}_{\alpha\mu\nu}$ is fully Bose symmetric. This is to be contrasted with the BQ^2 vertex, usually denoted by $\widetilde{\Gamma}_{\alpha\mu\nu}$, which is Bose symmetric only under the interchange of its two quantum legs. The SDE satisfied by $\widehat{\Gamma}_{\alpha\mu\nu}$ is shown in Fig. 1. Note that the tree-level expressions for $\Gamma_{\alpha\mu\nu}$ and $\widehat{\Gamma}_{\alpha\mu\nu}$ coincide:

$$\Gamma_{\alpha\mu\nu}^{(0)}(q, r, p) = \widehat{\Gamma}_{\alpha\mu\nu}^{(0)}(q, r, p) = (q-r)_\nu g_{\alpha\mu} + (r-p)_\alpha g_{\mu\nu} + (p-q)_\mu g_{\alpha\nu}. \quad (4.3)$$

For the purposes of the present work, the most important property of $\widehat{\Gamma}_{\alpha\mu\nu}$ is the fact that it satisfies the completely Bose-symmetric set of Abelian WIs

$$\begin{aligned} q^\alpha \widehat{\Gamma}_{\alpha\mu\nu}(q, r, p) &= p^2 \widehat{J}(p^2) P_{\mu\nu}(p) - r^2 \widehat{J}(r^2) P_{\mu\nu}(r), \\ r^\mu \widehat{\Gamma}_{\alpha\mu\nu}(q, r, p) &= q^2 \widehat{J}(q^2) P_{\alpha\nu}(q) - p^2 \widehat{J}(p^2) P_{\alpha\nu}(p), \\ p^\nu \widehat{\Gamma}_{\alpha\mu\nu}(q, r, p) &= r^2 \widehat{J}(r^2) P_{\alpha\mu}(r) - q^2 \widehat{J}(q^2) P_{\alpha\mu}(q). \end{aligned} \quad (4.4)$$

These simple WIs are to be contrasted with the STIs satisfied by $\Gamma_{\alpha\mu\nu}$, namely

$$q^\alpha \Gamma_{\alpha\mu\nu}(q, r, p) = F(q^2) [p^2 J(p^2) P_\nu^\alpha(p) H_{\alpha\mu}(p, q, r) - r^2 J(r^2) P_\mu^\alpha(r) H_{\alpha\nu}(r, q, p)] \quad (4.5)$$

and cyclic permutations. The tensorial decomposition of $H_{\nu\mu}$ is given by [35]

$$H_{\nu\mu}(p, r, q) = g_{\mu\nu} a_{qrp} - r_\mu q_\nu b_{qrp} + \overline{q}_\mu p_\nu c_{qrp} + q_\nu p_\mu d_{qrp} + p_\mu p_\nu e_{qrp}, \quad (4.6)$$

where a_{qrp} is short-hand notation for $a(q, r, p)$, etc.

An immediate consequence of Eq. (4.4) is the QED-like relation

$$\widehat{Z}_1 = \widehat{Z}_A. \quad (4.7)$$

between the wave-function renormalization for $\widehat{\Delta}$, introduced in Eq. (3.1), and the vertex renormalization defined as

$$\widehat{Z}_1 \widehat{\Gamma}^{\alpha\mu\nu}(q, r, p) = \widehat{\Gamma}_R^{\alpha\mu\nu}(q, r, p). \quad (4.8)$$

In addition, one may extract from the set of WIs given in Eq. (4.4) the expression of the vertex $\widehat{\Gamma}_{\alpha\mu\nu}$ in the kinematical limit $r \rightarrow 0$, which will be the relevant momentum configuration in the subsequent analysis (for a related analysis, see also [40]). To show that, consider the Taylor expansion of a function $f(q, r, p)$ around $r = 0$ (and $p = -q$). In general we have

$$f(q, r, p) = f(q, 0, -q) + r^\mu \left\{ \frac{\partial}{\partial r^\mu} f(q, r, p) \right\}_{r=0} + \mathcal{O}(r^2), \quad (4.9)$$

where the Lorentz structure of the function f has been suppressed. Specializing this result to the second WI in Eq. (4.4), one finds

$$\begin{aligned} r^\mu \widehat{\Gamma}_{\alpha\mu\nu}(q, r, p) &= r^\mu \widehat{\Gamma}_{\alpha\mu\nu}(q, 0, -q) + \mathcal{O}(r^2) \\ &= -r^\mu \left\{ \frac{\partial}{\partial r^\mu} \left[(q+r)^2 \widehat{J}(q+r) P_{\alpha\nu}(q+r) \right] \right\}_{r=0} + \mathcal{O}(r^2). \end{aligned} \quad (4.10)$$

where we have use the fact that the zero-th order term of Eq. (4.9) vanishes in this case. Thus, equating the coefficients of the terms linear in r^μ , one obtains the relation

$$\begin{aligned}\widehat{\Gamma}_{\alpha\mu\nu}(q, 0, -q) &= -\left\{\frac{\partial}{\partial r^\mu} \left[(q+r)^2 \widehat{J}(q+r) P_{\alpha\nu}(q+r) \right]\right\}_{r=0} \\ &= -\frac{\partial}{\partial q^\mu} \left[q^2 \widehat{J}(q^2) P_{\alpha\nu}(q) \right].\end{aligned}\quad (4.11)$$

Interestingly enough, the above relation is formally equivalent to the well-known QED text-book result

$$\Gamma_\mu(0, -p, p) = -\frac{\partial}{\partial p^\mu} S^{-1}(p), \quad (4.12)$$

obtained from the WI

$$q^\mu \Gamma_\mu(q, -q-p, p) = S^{-1}(p) - S^{-1}(q+p), \quad (4.13)$$

relating the photon-electron vertex with the electron propagator.

Next, the derivative of Eq. (4.11) can be easily evaluated by applying the formula

$$\begin{aligned}\frac{\partial}{\partial q^\mu} P_{\alpha\nu}(q) &= 2q_\mu \frac{q_\alpha q_\nu}{q^4} - \frac{1}{q^2} (g_{\mu\alpha} q_\nu + g_{\mu\nu} q_\alpha) \\ &= -\frac{1}{q^2} [q_\alpha P_{\mu\nu}(q) + q_\nu P_{\mu\alpha}(q)],\end{aligned}\quad (4.14)$$

yielding the final result

$$\begin{aligned}\widehat{\Gamma}_{\alpha\mu\nu}(q, 0, -q) &= \widehat{J}(q^2) (g_{\alpha\mu} q_\nu + g_{\nu\mu} q_\alpha - 2g_{\alpha\nu} q_\mu) - 2q^2 \widehat{J}'(q^2) q_\mu P_{\alpha\nu}(q) \\ &= \widehat{J}(q^2) \widehat{\Gamma}_{\alpha\mu\nu}^{(0)}(q, 0, -q) - 2q^2 \widehat{J}'(q^2) q_\mu P_{\alpha\nu}(q),\end{aligned}\quad (4.15)$$

where the prime indicates the derivative with respect to q^2 . Note that, due to Bose symmetry, the procedure described above can be applied exactly in the same way for the remaining WIs, in order to obtain the kinematical limits $q, p \rightarrow 0$ of the vertex $\widehat{\Gamma}_{\alpha\mu\nu}$. Also, we observe that the tensorial structure of the full vertex $\widehat{\Gamma}_{\alpha\mu\nu}$ in this particular kinematical limit is not exhausted by the term proportional to the tree level expression.

B. The pole part of the three-gluon vertex

As has been explained in a series of recent works, a crucial condition for obtaining an infrared finite gluon propagator, without interfering with the gauge invariance (or the BRST symmetry) of the theory, is the existence of a set of special vertices, to be generically denoted

by V , that are completely longitudinal and contain massless poles. The dynamical origin of the aforementioned poles is purely nonperturbative: for sufficiently strong binding, the mass of certain (colored) bound states may be reduced to zero [41–45].

The role of these vertices is two-fold. On the one hand, thanks to the massless poles they contain, they make possible the emergence of an infrared finite solution out of the SDE governing the gluon propagator; thus, one invokes essentially a non-Abelian realization of the well-known Schwinger mechanism [46, 47]. On the other hand, these same poles act like composite Nambu-Goldstone excitations, preserving the form of the STIs of the theory in the presence of a gluon mass.

Specifically, in order for the WIs to maintain the same form before and after mass generation, the effective substitution

$$\widehat{\Delta}^{-1}(q^2) = q^2 \widehat{J}(q^2) \longmapsto \widehat{\Delta}_m^{-1}(q^2) = q^2 \widehat{J}_m(q^2) - \widehat{m}^2(q^2), \quad (4.16)$$

implemented by the mass generation at the level the gluon propagator, must be accompanied by the simultaneous replacement of the vertex [29]

$$\widehat{\Gamma} \longmapsto \widehat{\Gamma}' = \widehat{\Gamma}_m + \widehat{V}. \quad (4.17)$$

Then, since

$$q^\alpha \widehat{\Gamma}_{m\alpha\mu\nu}(q, r, p) = p^2 \widehat{J}_m(p^2) P_{\mu\nu}(p) - r^2 \widehat{J}_m(r^2) P_{\mu\nu}(r), \quad (4.18)$$

$$q^\alpha \widehat{V}_{\alpha\mu\nu}(q, r, p) = \widehat{m}^2(r^2) P_{\mu\nu}(r) - \widehat{m}^2(p^2) P_{\mu\nu}(p), \quad (4.19)$$

one finds that the corresponding WI satisfied by $\widehat{\Gamma}'$ would read

$$\begin{aligned} q^\alpha \widehat{\Gamma}'_{\alpha\mu\nu}(q, r, p) &= q^\alpha \left[\widehat{\Gamma}_m(q, r, p) + \widehat{V}(q, r, p) \right]_{\alpha\mu\nu} \\ &= [p^2 \widehat{J}_m(p^2) - \widehat{m}^2(p^2)] P_{\mu\nu}(p) - [r^2 \widehat{J}_m(r^2) - \widehat{m}^2(r^2)] P_{\mu\nu}(r) \\ &= \widehat{\Delta}_m^{-1}(p^2) P_{\mu\nu}(p) - \widehat{\Delta}_m^{-1}(r^2) P_{\mu\nu}(r), \end{aligned} \quad (4.20)$$

which is indeed the first of the identities in Eq. (4.4), with the aforementioned replacement $\widehat{\Delta}^{-1} \rightarrow \widehat{\Delta}_m^{-1}$ enforced.

The closed expression for $\widehat{V}_{\alpha\mu\nu}$ may be reconstructed from the WIs it satisfies (namely Eq. (4.19) and its cyclic permutations), together with the condition of complete longitudinality, *i.e.*,

$$P^{\alpha'\alpha}(q) P^{\mu'\mu}(r) P^{\nu'\nu}(p) \widehat{V}_{\alpha'\mu'\nu'}(q, r, p) = 0; \quad (4.21)$$

it reads,

$$\widehat{V}_{\alpha\mu\nu}(q, r, p) = \frac{q_\alpha}{q^2}[\widehat{m}^2(r^2) - \widehat{m}^2(p^2)]P_\mu^\rho(r)P_{\rho\nu}(p) + \text{c.p.}, \quad (4.22)$$

where c.p. denotes ‘‘cyclic permutations’’. As we will see in the next section, due to its completely longitudinal nature [*viz.* Eq. (4.21)], the contribution of this pole vertex to the typical lattice ratio, given in Eq. (5.3), vanishes in the Landau gauge.

C. The longitudinal form factors

The complete closed form of $\widehat{\Gamma}_m$ is not known; its longitudinal part, however, may be reconstructed from the WIs that $\widehat{\Gamma}_m$ satisfies, following rather standard procedures [35]. Specifically, one begins by separating the vertex into the ‘‘longitudinal’’ and the (totally) ‘‘transverse’’ parts,

$$\widehat{\Gamma}_m^{\alpha\mu\nu}(q, r, p) = \widehat{\Gamma}_{m(\ell)}^{\alpha\mu\nu}(q, r, p) + \widehat{\Gamma}_{m(t)}^{\alpha\mu\nu}(q, r, p), \quad (4.23)$$

where the component $\widehat{\Gamma}_{m(\ell)}$ satisfies the WI of Eq. (4.18) (and its permutations), whereas $q_\alpha \widehat{\Gamma}_{m(t)}^{\alpha\mu\nu}(q, r, p) = r_\mu \widehat{\Gamma}_{m(t)}^{\alpha\mu\nu}(q, r, p) = p_\nu \widehat{\Gamma}_{m(t)}^{\alpha\mu\nu}(q, r, p) = 0$.

The longitudinal part is then decomposed into 10 form factors \widehat{X}_i , according to

$$\widehat{\Gamma}_{m(\ell)}^{\alpha\mu\nu}(q, r, p) = \sum_{i=1}^{10} \widehat{X}_i(q, r, p) \ell_i^{\alpha\mu\nu}, \quad (4.24)$$

with the explicit form of the tensors ℓ^i given by [31]

$$\begin{aligned} \ell_1^{\alpha\mu\nu} &= (q-r)^\nu g^{\alpha\mu} & \ell_2^{\alpha\mu\nu} &= -p^\nu g^{\alpha\mu} & \ell_3^{\alpha\mu\nu} &= (q-r)^\nu [q^\mu r^\alpha - (q \cdot r) g^{\alpha\mu}] \\ \ell_4^{\alpha\mu\nu} &= (r-p)^\alpha g^{\mu\nu} & \ell_5^{\alpha\mu\nu} &= -q^\alpha g^{\mu\nu} & \ell_6^{\alpha\mu\nu} &= (r-p)^\alpha [r^\nu p^\mu - (r \cdot p) g^{\mu\nu}] \\ \ell_7^{\alpha\mu\nu} &= (p-q)^\mu g^{\alpha\nu} & \ell_8^{\alpha\mu\nu} &= -r^\mu g^{\alpha\nu} & \ell_9^{\alpha\mu\nu} &= (p-q)^\mu [p^\alpha q^\nu - (p \cdot q) g^{\alpha\nu}] \\ \ell_{10}^{\alpha\mu\nu} &= q^\nu r^\alpha p^\mu + q^\mu r^\nu p^\alpha. \end{aligned} \quad (4.25)$$

Then, the WI of Eq. (4.18) and its permutations give rise to an algebraic system for the \widehat{X}_i , whose solution reads,

$$\begin{aligned} \widehat{X}_1 &= \frac{1}{2}[\widehat{J}_m(q^2) + \widehat{J}_m(r^2)], & \widehat{X}_2 &= \frac{1}{2}[\widehat{J}_m(q^2) - \widehat{J}_m(r^2)], & \widehat{X}_3 &= \frac{\widehat{J}_m(q^2) - \widehat{J}_m(r^2)}{q^2 - r^2}, \\ \widehat{X}_4 &= \frac{1}{2}[\widehat{J}_m(r^2) + \widehat{J}_m(p^2)], & \widehat{X}_5 &= \frac{1}{2}[\widehat{J}_m(r^2) - \widehat{J}_m(p^2)], & \widehat{X}_6 &= \frac{\widehat{J}_m(r^2) - \widehat{J}_m(p^2)}{r^2 - p^2}, \\ \widehat{X}_7 &= \frac{1}{2}[\widehat{J}_m(p^2) + \widehat{J}_m(q^2)], & \widehat{X}_8 &= \frac{1}{2}[\widehat{J}_m(p^2) - \widehat{J}_m(q^2)], & \widehat{X}_9 &= \frac{\widehat{J}_m(p^2) - \widehat{J}_m(q^2)}{p^2 - q^2}, \\ \widehat{X}_{10} &= 0. \end{aligned} \quad (4.26)$$

Thus, the longitudinal form factors of $\widehat{\Gamma}_{m(\ell)}^{\alpha\mu\nu}(q, r, p)$ involve *only* the quantity \widehat{J}_m , since it is the only quantity that enters on the rhs of Eq. (4.18). Instead, the corresponding expressions for the form factors of the conventional (Q^3) vertex, $\Gamma^{\alpha\mu\nu}$, first derived in [35], contain, in addition, the ghost dressing function F and the various form-factors comprising the gluon-ghost kernel $H_{\mu\nu}$. For example, the closed form of X_7 (to be employed in the next section) is given by

$$\begin{aligned} X_7(q, r, p) = & \frac{1}{4} \{ 2[F(q)J_m(p)a_{rqp} + F(p)J_m(q)a_{rpq}] + r^2[F(p)J_m(r)b_{qpr} + F(q)J_m(r)b_{pqr}] \\ & + (q^2 - p^2)[F(r)J_m(q)b_{prq} + F(q)J_m(p)b_{rqp} - F(r)J_m(p)b_{qrp} - F(p)J_m(q)b_{rpq}] \\ & + 2(qr)F(p)J_m(q)d_{rqp} + 2(rp)F(q)J(p)d_{rqp} \}. \end{aligned} \quad (4.27)$$

Note in addition, that, unlike \widehat{X}_{10} , the corresponding X_{10} does not vanish.

Finally, the (undetermined) transverse part of the vertex is described by the remaining 4 form factors \widehat{Y}_i ,

$$\widehat{\Gamma}_{m(t)}^{\alpha\mu\nu}(q, r, p) = \sum_{i=1}^4 \widehat{Y}_i(q, r, p) t_i^{\alpha\mu\nu}, \quad (4.28)$$

with the completely transverse tensors t^i given by

$$\begin{aligned} t_1^{\alpha\mu\nu} &= [(q \cdot r)g^{\alpha\mu} - q^\mu r^\alpha][(r \cdot p)q^\nu - (q \cdot p)r^\nu] \\ t_2^{\alpha\mu\nu} &= [(r \cdot p)g^{\mu\nu} - r^\nu p^\mu][(p \cdot q)r^\alpha - (r \cdot q)p^\alpha] \\ t_3^{\alpha\mu\nu} &= [(p \cdot q)g^{\nu\alpha} - p^\alpha q^\nu][(q \cdot r)p^\mu - (r \cdot p)q^\mu] \\ t_4^{\alpha\mu\nu} &= g^{\mu\nu}[(p \cdot q)r^\alpha - (r \cdot q)p^\alpha] + g^{\alpha\mu}[(r \cdot p)q^\nu - (q \cdot p)r^\nu] + g^{\alpha\nu}[(r \cdot q)p^\mu - (r \cdot p)q^\mu] \\ &+ p^\alpha q^\mu r^\nu - r^\alpha p^\mu q^\nu. \end{aligned} \quad (4.29)$$

It turns out that in the limit $r \rightarrow 0$ all the transverse tensors in Eq. (4.29) are zero, so the transverse part of the vertex vanishes in this limit. On the other hand, for the same limit, only the following longitudinal tensors given in Eq. (4.25) survive

$$\begin{aligned} \ell_1^{\alpha\mu\nu} &= q^\nu g^{\alpha\mu} & \ell_2^{\alpha\mu\nu} &= q^\nu g^{\alpha\mu} & \ell_4^{\alpha\mu\nu} &= q^\alpha g^{\mu\nu} \\ \ell_5^{\alpha\mu\nu} &= -q^\alpha g^{\mu\nu} & \ell_7^{\alpha\mu\nu} &= -2q^\mu g^{\alpha\nu} & \ell_9^{\alpha\mu\nu} &= -2q^2 q^\mu P^{\alpha\nu}(q), \end{aligned} \quad (4.30)$$

with the associated form factors

$$\begin{aligned} \widehat{X}_1 &= \frac{1}{2}[\widehat{J}(q^2) + \widehat{J}(0)], & \widehat{X}_2 &= \frac{1}{2}[\widehat{J}(q^2) - \widehat{J}(0)], & \widehat{X}_4 &= \frac{1}{2}[\widehat{J}(0) + \widehat{J}(q^2)], \\ \widehat{X}_5 &= \frac{1}{2}[\widehat{J}(0) - \widehat{J}(q^2)], & \widehat{X}_7 &= \widehat{J}(q^2), & \widehat{X}_9 &= \widehat{J}(q^2), \end{aligned} \quad (4.31)$$

corresponding to the limit $r \rightarrow 0$ of those appearing in Eq. (4.26). Thus, using these results, it is elementary to show that one is able to reproduce the expression given in Eq. (4.15).

V. LATTICE PROSPECTS

In this section we first discuss the theoretical possibilities of simulating PT-BFM Green's functions on the lattice. Then, we consider the relevant lattice quantity, and derive its general expression in terms of the various (longitudinal and transverse) form factors. Next, we show how the effective charge and gluon mass may be reconstructed from the data obtained in a standard kinematical limit. In addition, we present a numerical study on the propagation of the (modeled) data errors into the effective charge and gluon mass. Finally, exploiting some basic field-theoretic properties, we relate the conventional and BFM lattice quantity at the origin.

A. BFM on the lattice

Within perturbation theory, the BFM was formulated to all orders on the lattice in [48] (see also the early work of Gross and Dashen [49]); however, its nonperturbative implementation has been pending for quite some time. A possible nonperturbative formulation, which evades the well-known “Neuberger 0/0 problem” [50], has been only recently introduced in [32], through a reformulation of the BFM method in terms of canonical transformations (so that dynamical ghosts are not needed). This led to the proposal of the gauge fixing functional [32, 33]

$$F[g] = - \int d^4x \text{Tr} (A_\mu^g - \widehat{A}_\mu)^2, \quad (5.1)$$

which upon minimization on the group elements g provides the background Landau gauge condition $\widehat{\mathcal{D}}_\mu(A_\mu^g - \widehat{A}_\mu) = 0$. Then, on the minimum of this functional, the mapping given by

$$A \rightarrow A^{g(A, \widehat{A})} - \widehat{A} \equiv Q_\mu \quad (5.2)$$

defines the action of a canonical transformation on the gauge fields, constituting a non-perturbative generalization of the familiar splitting into a background and a quantum field [51]. The inverse of this mapping amounts to a gauge transformation, which can be used to determine the quantum field Q corresponding to the gauge configuration minimizing the

gauge-fixing functional (5.1). The relevant correlators (*e.g.*, in the two- and three-point functions) may then be constructed in terms of this particular field, and lattice simulations of the corresponding discretized version can be then carried out.

Preliminary numerical simulations for a variety of explicit backgrounds have been performed in [33], indicating that the functional (5.1) furnishes a convergence rate comparable to that of the zero background case. Note, however, that in the PT-BFM formulation one considers the background field as an external yet unspecified source, to be set to zero after taking the appropriate derivatives of the vertex functional. Therefore, in order to properly simulate this procedure on the lattice, one ought to introduce a suitable dependence of the background field \widehat{A} on a parameter, which, upon variation, would smoothly turn it off. Work in this direction is already in progress; at the moment, we are not aware of any theoretical obstruction that would prevent the computation of PT-BFM Green's functions on the lattice by techniques similar to those discussed in [52].

B. The basic lattice quantity

Let us therefore assume that the three-point function defined in Eq. (4.1) may be indeed simulated on the lattice, following the procedure briefly outlined above. Then, as is customary, in the Landau gauge, one considers the following ratio [36]

$$\widehat{R}(q, r, p) = \frac{\mathcal{N}(q, r, p)}{\mathcal{D}(q, r, p)}, \quad (5.3)$$

with the numerator and denominator given by

$$\begin{aligned} \mathcal{N}(q, r, p) &= \Gamma_{\alpha\mu\nu}^{(0)}(q, r, p) \widehat{\mathcal{G}}_{\rho\sigma\tau}(q, r, p), \\ \mathcal{D}(q, r, p) &= \Gamma_{\alpha\mu\nu}^{(0)}(q, r, p) P^{\alpha\rho}(q) P^{\mu\sigma}(r) P^{\nu\tau}(p) \Gamma_{\rho\sigma\tau}^{(0)}(q, r, p) \widehat{\Delta}_m(q) \widehat{\Delta}_m(r) \widehat{\Delta}_m(p), \end{aligned} \quad (5.4)$$

where a common color factor cancels out in the ratio. Note the index “m” in the full propagators, indicating the nonperturbative generation of a gluon mass. In addition, and according to the discussion in the previous section, the substitution given in Eq. (4.17) must also be implemented. Then, inserting Eq. (4.2) into $\mathcal{N}(q, r, p)$, together with the aforementioned substitution, we see that (*i*) the product $\widehat{\Delta}_m(q) \widehat{\Delta}_m(r) \widehat{\Delta}_m(p)$ cancels out when forming the ratio of Eq. (5.3), and (*ii*) any reference to the pole vertex $\widehat{V}_{\rho\sigma\tau}$ disappears, due to the longitudinality condition Eq. (4.21) that it satisfies.

Thus, the numerator and denominator become

$$\begin{aligned}\mathcal{N}(q, r, p) &= \Gamma_{\alpha\mu\nu}^{(0)}(q, r, p)P_\rho^\alpha(q)P_\sigma^\mu(r)P_\tau^\nu(p)\widehat{\Gamma}_m^{\rho\sigma\tau}(q, r, p), \\ \mathcal{D}(q, r, p) &= \Gamma_{\alpha\mu\nu}^{(0)}(q, r, p)P^{\alpha\rho}(q)P^{\mu\sigma}(r)P^{\nu\tau}(p)\Gamma_{\rho\sigma\tau}^{(0)}(q, r, p).\end{aligned}\quad (5.5)$$

When one decomposes the full three-gluon vertex into a longitudinal and a transverse part, as in Eq. (4.23), the numerator in Eq. (5.5) becomes

$$\mathcal{N}(q, r, p) = \mathcal{N}_{(\ell)}(q, r, p) + \mathcal{N}_{(t)}(q, r, p), \quad (5.6)$$

with

$$\mathcal{N}_{(\ell,t)}(q, r, p) = \Gamma_{\alpha\mu\nu}^{(0)}(q, r, p)P_\rho^\alpha(q)P_\sigma^\mu(r)P_\tau^\nu(p)\widehat{\Gamma}_{m,(\ell,t)}^{\rho\sigma\tau}(q, r, p). \quad (5.7)$$

Then, the denominator is given by

$$\mathcal{D}(q, r, p) = 4\frac{r^2p^2 - (r\cdot p)^2}{q^2r^2p^2}[3(q^2r^2 + q^2p^2 + r^2p^2) + (r\cdot p)^2 - r^2p^2], \quad (5.8)$$

the longitudinal part of the numerator by

$$\begin{aligned}\mathcal{N}_{(\ell)}(q, r, p) &= 4\frac{r^2p^2 - (rp)^2}{q^2r^2p^2} \left\{ [3q^2r^2 - (q\cdot p)(p\cdot r)]\widehat{A}_1 + [3r^2p^2 - (p\cdot q)(q\cdot r)]\widehat{A}_2 \right. \\ &\quad \left. + [3q^2p^2 - (q\cdot r)(r\cdot p)]\widehat{A}_3 + [(q\cdot r)(r\cdot p)(p\cdot q) - q^2r^2p^2]\widehat{A}_4 \right\},\end{aligned}\quad (5.9)$$

and its transverse part by

$$\begin{aligned}\mathcal{N}_{(t)}(q, r, p) &= 2[r^2p^2 - (rp)^2] \left\{ [3(q\cdot r) - p^2]\widehat{Y}_1 + [3(r\cdot p) - q^2]\widehat{Y}_2 \right. \\ &\quad \left. + [3(q\cdot p) - r^2]\widehat{Y}_3 + 6\widehat{Y}_4 \right\}.\end{aligned}\quad (5.10)$$

Note also that the identity

$$(q\cdot r)(r\cdot p) + (r\cdot p)(p\cdot q) + (p\cdot q)(q\cdot r) = q^2r^2 - (q\cdot r)^2 = q^2p^2 - (q\cdot p)^2 = r^2p^2 - (r\cdot p)^2, \quad (5.11)$$

which can be easily proved using momentum conservation, has been employed in deriving the above expressions, and that we have introduced the notation

$$\begin{aligned}\widehat{A}_1 &= \widehat{X}_1 - (q\cdot r)\widehat{X}_3; & \widehat{A}_2 &= \widehat{X}_4 - (r\cdot p)\widehat{X}_6; \\ \widehat{A}_3 &= \widehat{X}_7 - (p\cdot q)\widehat{X}_9; & \widehat{A}_4 &= -\widehat{X}_3 - \widehat{X}_6 - \widehat{X}_9.\end{aligned}\quad (5.12)$$

It is important to emphasize that the expressions given in Eqs. (5.9) and (5.10) carry over directly to the case of the conventional three-gluon vertex $\Gamma_m^{\alpha\mu\nu}$, simply by converting

the hatted quantities to normal ones. Of course, as already mentioned, the functional form of the corresponding X_i comprising the A_i is significantly more complicated. Note also that even though X_{10} does not vanish, it still does not contribute to Eq. (5.9), because $P_\rho^\alpha(q)P_\sigma^\mu(r)P_\tau^\nu(p)\ell_{10}^{\rho\sigma\tau} = 0$.

It turns out that the physical quantity of interest may be extracted from \widehat{R} by employing a very common kinematic choice. Specifically, to begin with, as is customary in lattice studies, we will describe the ratio \widehat{R} in terms of the modulo of two independent momenta (say, q^2 and r^2) and the angle ϕ formed between them; thus $\widehat{R} = \widehat{R}(q^2, r^2, \phi)$. Then, the quantity of interest corresponds to the case $\widehat{R}(q^2, 0, \pi/2)$, which is a special case of the so-called ‘‘orthogonal configuration’’, namely $\widehat{R}(q^2, r^2, \pi/2)$.

In this latter configuration we have,

$$p^2 = q^2 + r^2; \quad q \cdot r = 0; \quad q \cdot p = -q^2; \quad r \cdot p = -r^2, \quad (5.13)$$

and, therefore, the relevant quantities reduce to

$$\mathcal{D}(q, r, \pi/2) = \frac{4}{q^2 + r^2} [3(q^4 + r^4) + 8q^2r^2], \quad (5.14)$$

and

$$\begin{aligned} \mathcal{N}^{(\ell)}(q, r, \pi/2) &= \frac{4}{q^2 + r^2} [2q^2r^2\widehat{A}_1 + 3r^2(q^2 + r^2)\widehat{A}_2 + 3q^2(q^2 + r^2)\widehat{A}_3 - q^2r^2(q^2 + r^2)\widehat{A}_4], \\ \mathcal{N}^{(t)}(q, r, \pi/2) &= -2q^2r^2[(q^2 + r^2)\widehat{Y}_1 + (3r^2 + q^2)\widehat{Y}_2 + (3q^2 + r^2)\widehat{Y}_3 + 6\widehat{Y}_4], \end{aligned} \quad (5.15)$$

with the (suppressed) arguments of the form-factors \widehat{A}_i and \widehat{Y}_i correspondingly adapted to the particular kinematic configuration chosen.

At this point, if, in addition, we set $r^2 = 0$, then *the transverse term vanishes*, $\mathcal{N}^{(t)}(q, 0, \pi/2) = 0$, and we obtain

$$\widehat{R}(q^2, 0, \pi/2) = \widehat{A}_3(q, 0, \pi/2) = \widehat{X}_7 + q^2\widehat{X}_9, \quad (5.16)$$

so that (we only indicate the q^2 in the argument of \widehat{R})

$$\widehat{R}(q^2) = [q^2\widehat{J}_m(q^2)]', \quad (5.17)$$

where, as before, the prime indicates derivatives with respect to q^2 . Let us point out that this particular result may be derived directly from Eq. (5.3), by substituting in it the expression

for $\widehat{\Gamma}_{\alpha\mu\nu}$ given in Eq. (4.15). Specifically,

$$\widehat{R}(q, r, p) = \widehat{J}(q^2) - 2q^2 \widehat{J}'(q^2) \left\{ \frac{\Gamma_{\alpha\mu\nu}^{(0)}(q, r, p) P^{\alpha\tau}(q) P_\sigma^\mu(r) P_\tau^\nu(p) q^\sigma}{\mathcal{D}(q, r, p)} \right\}. \quad (5.18)$$

In the orthogonal configuration ($q \cdot r = 0$), we have that $q^\sigma P_\sigma^\mu(r) = q^\mu$; then, using Eq. (5.14) and setting $r^2 = 0$, it is easy to show that the quantity in curly brackets is equal to $\{-\frac{1}{2}\}$.

Then, simple integration of Eq. (5.17) yields

$$q^2 \widehat{J}_m(q^2) = \int_0^{q^2} dp^2 \widehat{R}(p^2) + C, \quad (5.19)$$

and, assuming that both $\widehat{J}_m(q^2)$ and $\widehat{R}(p^2)$ are finite for all values of the momentum, we see that the integration constant must vanish, $C = 0$. Thus, finally, one obtains the relation

$$\widehat{J}_m(q^2) = \frac{1}{q^2} \int_0^{q^2} dp^2 \widehat{R}(p^2). \quad (5.20)$$

Let us next renormalize this result within the MOM scheme, denoting the final answer by $\widehat{J}_m^{(r)}(q^2)$. If we impose the standard MOM condition $\widehat{J}_m^{(r)}(\mu^2) = 1$, at some arbitrary momentum scale μ , then, we have that

$$\widehat{J}_m^{(r)}(q^2) = \frac{\widehat{J}_m(q^2)}{\widehat{J}_m(\mu^2)}. \quad (5.21)$$

However, let us point out that, strictly speaking, due to the presence of the gluon mass, this last normalization condition imposed on \widehat{J}_m cannot be enforced simultaneously with the corresponding MOM condition for $\widehat{\Delta}_m^{-1}(q^2)$, namely $\widehat{\Delta}_m^{-1}(\mu^2) = 1$. Indeed, since, for any arbitrary μ , $\widehat{\Delta}_m^{-1}(\mu^2) = \mu^2 \widehat{J}_m(\mu^2) + \widehat{m}^2(\mu^2)$, if at a given μ we impose that $\widehat{J}_m(\mu^2) = 1$, then, automatically, at the same μ , $\widehat{\Delta}_m^{-1}(\mu^2) = \mu^2 [1 + \widehat{m}^2(\mu^2)/\mu^2]$. Note however, that unless one chooses to push the value of μ very deep in the infrared, this discrepancy is numerically immaterial; for example, when one renormalizes $\widehat{\Delta}_m$ at $\mu = 4.3$ GeV, the value of the gluon mass at the origin is $\widehat{m}(0) = 1$ GeV, making the ratio $\widehat{m}^2(0)/\mu^2$ of the order of 5%. Of course, this estimate is just an upper bound for the relevant ratio $m^2(\mu^2)/\mu^2$, which in reality is significantly smaller, since the function $\widehat{m}^2(q^2)$ is decreasing rather rapidly (see, *e.g.*, the inset of the left panel of Fig. 2); in fact, at $\mu = 4.3$ GeV, the gluon mass is practically negligible.

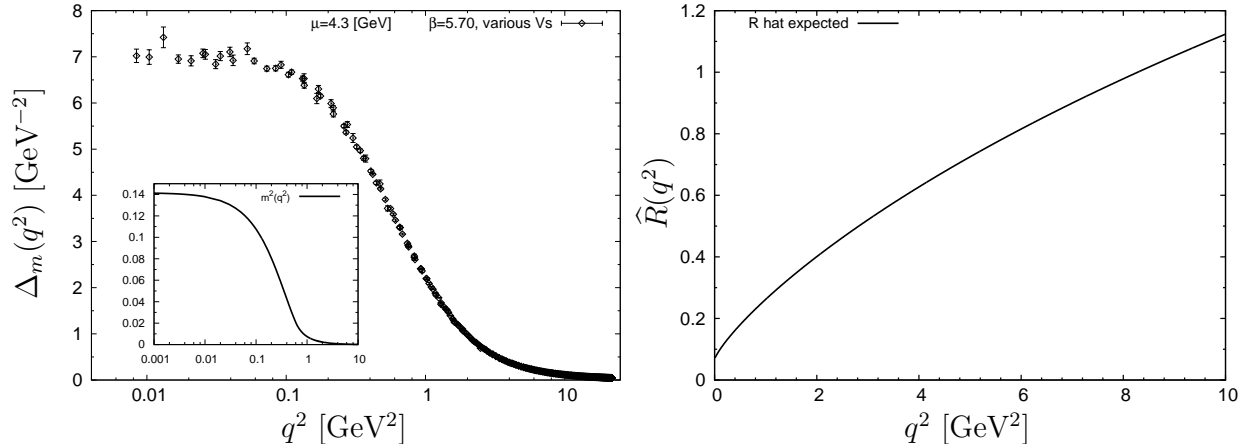


FIG. 2: The expected shape of the ratio $\widehat{R}(q^2)$ (right panel), obtained starting from the quenched lattice data for the $SU(3)$ gluon propagator $\Delta_m(q^2)$ (left panel), and the corresponding solution of the mass equation $m^2(q^2)$ (left panel, inset).

C. Modelling the error propagation

In order to understand how a possible lattice signal for the quantity $\widehat{R}(q^2)$ of Eq. (5.17) may provide direct information on the effective charge $\bar{\alpha}(q^2)$ (and the possible caveats associated with such a determination), we perform in what follows a detailed numerical study. Specifically, starting from the knowledge of the conventional quenched lattice propagator $\Delta_m(q^2)$ and ghost dressing function $F(q^2)$ [3], together with the associated solution of the mass equation $m^2(q^2)$ [30], one can reconstruct first $\widehat{J}(q^2)$, and next obtain the expected shape of $\widehat{R}(q^2)$ through

$$\widehat{R}(q^2) = \left[\frac{\Delta_m^{-1}(q^2) - m^2(q^2)}{F^2(q^2)} \right]', \quad (5.22)$$

where we have used Eq. (2.6) in Euclidean space.

The resulting curve (shown in Fig. 2), which will be referred to as the ‘expected’ result, can be parametrized to a high precision by the function

$$\widehat{R}(q^2) = A_2 + \frac{A_1 - A_2}{1 + (q^2/q_0^2)^{\bar{x}}}, \quad (5.23)$$

with best fit parameters corresponding to the values

$$\bar{A}_1 = 0.083; \quad \bar{A}_2 = 5.150; \quad \bar{q}_0 = 7.156 \text{ GeV}; \quad \bar{x} = 0.836. \quad (5.24)$$

The above functional form of the expected behavior of $\widehat{R}(q^2)$ is rather useful, because it allows for a systematic analysis of how uncertainties, simulated through deviations of

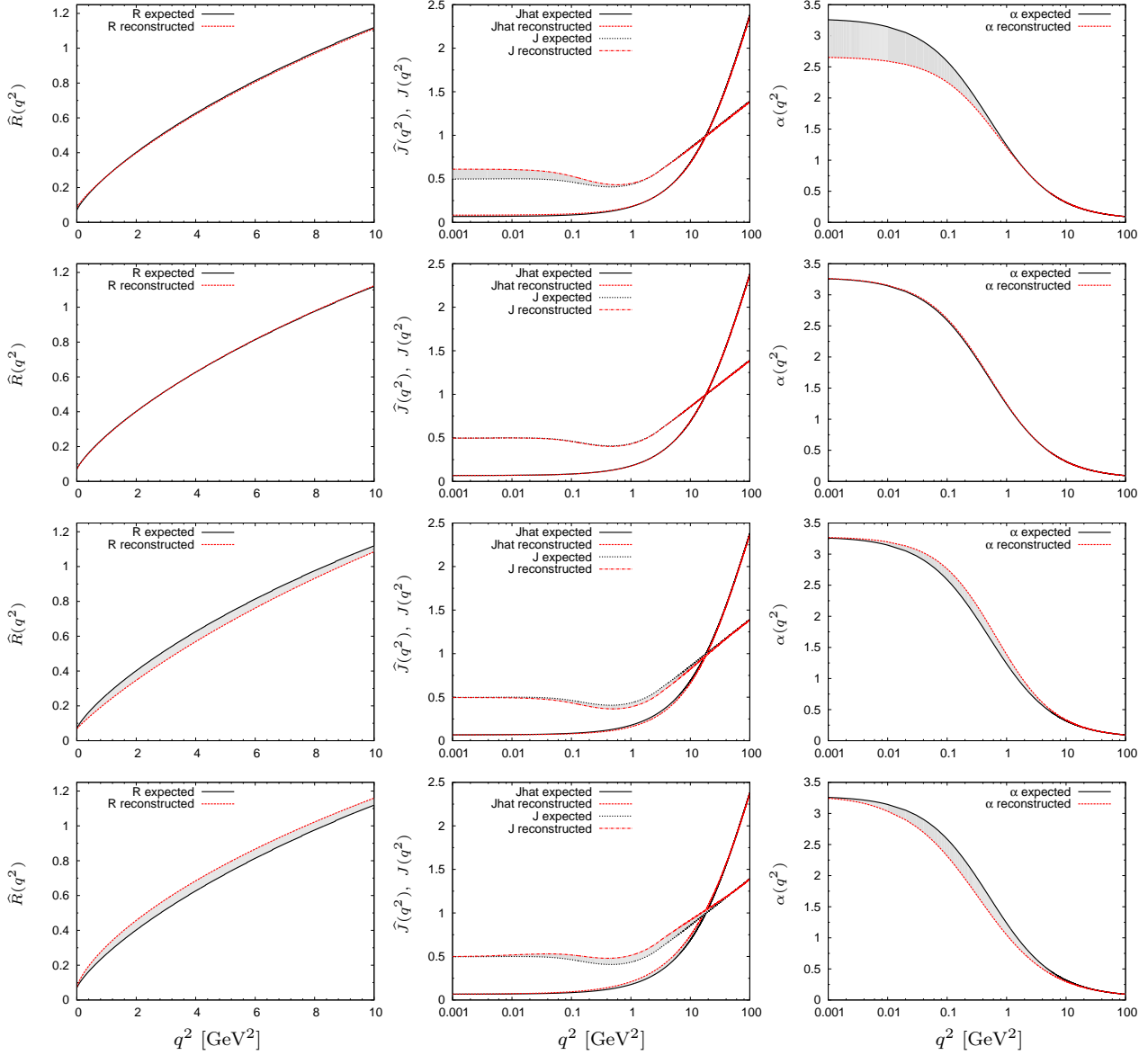


FIG. 3: (color online) Numerical study of how uncertainties in the determination of $\widehat{R}(q^2)$, parametrized according to Eq. (5.23), reflect into the determination of \widehat{J} , J as well as the effective charge $\overline{\alpha}(q^2)$. In particular, we compare the ‘expected’ results with the results reconstructed from the parametrization (5.23) for the following parameter values: (first row) the best fit parameters (5.24); (second row) A_1 fixed at the expected value $\widehat{R}(0) = 0.0562$, and, for the remaining coefficients the refitted values $A_2 = 5.246$, $q_0 = 7.279$ and $x = 0.8167$; (third row) A_1 and x fixed at the values $\widehat{R}(0)$ and 0.92 respectively, and $A_2 = 4.632$, $q_0 = 6.234$ GeV ; (fourth row) A_1 and x fixed at the values $\widehat{R}(0)$ and $x = 0.72$ respectively, and, finally, $A_2 = 6.251$ $q_0 = 9.21$ GeV.

the fitting parameters from their “optimal” values, can influence the reconstruction of the

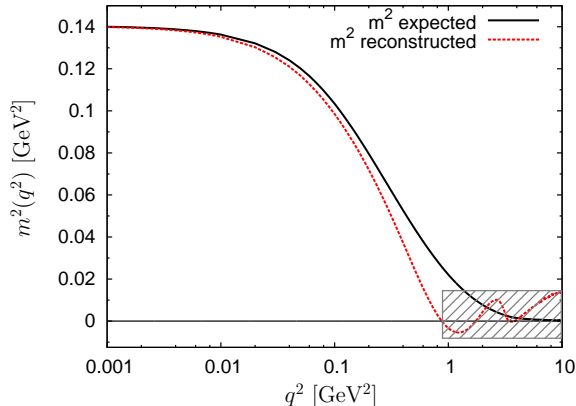


FIG. 4: The reconstructed running mass starting from $\widehat{R}(q^2)$ as given in Eq. (5.23) when the parameters chosen are the best fit ones of Eq. (5.24). Notice the problems that afflict the determination of the UV mass tail (shaded region).

effective charge (and gluon mass, see below).

The results of this study are shown in Fig. 3. As can be seen, the most sizable deviation between the ‘expected’ and the reconstructed results occurs when uncertainties in the determination of $\widehat{R}(0)$ are sizable (Fig. 3, first row). This is mainly due to the fact that the ‘expected’ value for $\widehat{R}(0)$ turns out to be of $\mathcal{O}(10^{-2})$, and moderate deviations imply a considerable effect in the determination of \widehat{J}_m through Eq. (5.20); this, in turn, translates into a large variation of the effective charge, given that $\bar{\alpha} \sim \widehat{J}_m^{-1}$, see Eq. (3.5).

Specifically, in the first row of Fig. 3 we show the results for \widehat{R} , \widehat{J} , J and $\bar{\alpha}$ obtained starting from Eq. (5.23) with the best fit parameters (5.24); since in the parametrization (5.23), $\widehat{R}(0) \equiv \bar{A}_1$, such fit overestimates the value at the origin; this error propagates in the determination of a reconstructed effective charge, which comes out suppressed in the IR with respect to the ‘expected’ value.

The following three rows in Fig. 3 show the effect of uncertainties in the determination of the exponent x (which controls the overall shape of the \widehat{R} curve), once the behavior at the origin has been fixed to its ‘expected’ value, that is A_1 is fixed to the value $\widehat{R}(0)$. As can be seen, the effect is significantly milder, and one can always reconstruct the effective charge to a high degree of accuracy.

Finally, let us focus our attention to the mass $m^2(q^2)$; as we will see, its reconstruction from this particular type of lattice measurements is especially subtle. The main difficulty

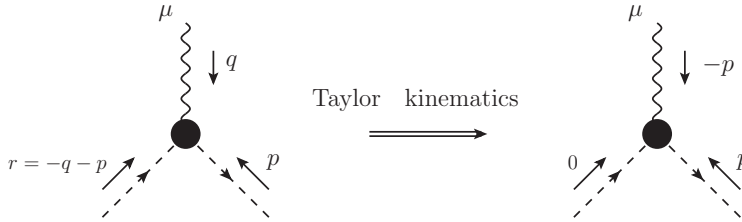


FIG. 5: The ghost-gluon vertex and the Taylor kinematics.

stems from the fact that the extraction of $m^2(q^2)$ proceeds by means of the relation

$$m^2(q^2) = \Delta_m^{-1}(q^2) - q^2 J_m(q^2). \quad (5.25)$$

Now, whereas both terms on the rhs increase in the UV, on theoretical grounds we know that $m^2(q^2)$ must decrease rather rapidly; this, in turn, implies that a rather delicate cancellation between these aforementioned two terms must take place. This cancellation, however, is very likely to be distorted by the reconstruction procedure, especially for high values of q^2 . This particular problem is shown in Fig. 4, where we plot the reconstructed mass for $\widehat{R}(q^2)$ provided by Eqs. (5.23) and (5.24). As can be seen there, while the determination in the IR is reasonably accurate, the tail is seriously distorted, displaying even negative regions. This characteristic pathology persists (with various degrees of intensity) in all cases analyzed in Fig. 3.

D. Relating $\widehat{R}(0)$ with $R(0)$

Let us now consider the conventional $R(q^2)$, obtained from Eq. (5.16) through the direct substitution $\widehat{X}_{7,9} \rightarrow X_{7,9}$. Obviously, the complicated structure of X_7 and X_9 [see, e.g., Eq. (4.27)], infested by the unknown form factors of the ghost-gluon kernel, makes their use for arbitrary q^2 impractical. However, when $q^2 = 0$ the corresponding expressions simplify substantially, providing a fairly simple expression for $R(0)$.

Specifically, after implementing $\widehat{X}_{7,9} \rightarrow X_{7,9}$ in Eq. (5.16), let us set $q^2 = 0$, to obtain

$$R(0) = F(0)J_m(0)a(0, 0, 0), \quad (5.26)$$

where Eq. (4.27) has been employed.

At this point one may invoke Taylor's theorem [53] in order to determine, under mild assumptions, the value of $a(0, 0, 0)$. To that end, consider the general Lorentz decomposition

for the ghost-gluon vertex,

$$\Gamma_\mu(r, q, p) = B_1(r, q, p)q_\mu - B_2(r, q, p)p_\mu. \quad (5.27)$$

Notice that, setting $B_1^{(0)} = 0$ and $B_2^{(0)} = 1$, one recovers the tree-level value of the ghost-gluon vertex $\Gamma_\mu^{(0)} = -p_\mu$. In the Taylor kinematic configuration, see Fig. 5, Eq. (5.27) becomes

$$\Gamma_\mu(0, -p, p) = -[B_1(0, -p, p) + B_2(0, -p, p)]p_\mu. \quad (5.28)$$

Taylor's theorem states that

$$B_1(0, -p, p) + B_2(0, -p, p) = 1, \quad (5.29)$$

to all-orders in perturbation theory.

On the other hand, it is well-known that $\Gamma_\mu(r, q, p)$ can be obtained from the contraction

$$\begin{aligned} \Gamma_\mu(r, q, p) &= -p^\nu H_{\nu\mu}(p, r, q) \\ &= -[a_{qrp} + (q \cdot p)b_{qrp} + (q \cdot p)d_{qrp} + p^2 e_{qrp}]p_\mu - [(q \cdot p)b_{qrp} + p^2 c_{qrp}]q_\mu, \end{aligned} \quad (5.30)$$

which, in the Taylor kinematics reduces to

$$\Gamma_\mu(0, -p, p) = -\{a(-p, 0, p) - p^2[c(-p, 0, p) + d(-p, 0, p) - e(-p, 0, p)]\}p_\mu. \quad (5.31)$$

Thus, equating Eq. (5.28) with Eq. (5.31) and using Eq. (5.29), we deduce the constraint

$$a(-p, 0, p) - p^2[c(-p, 0, p) + d(-p, 0, p) - e(-p, 0, p)] = 1. \quad (5.32)$$

Finally, taking the limit $p \rightarrow 0$ in Eq. (5.32), and assuming that c, d , and e are regular functions in that limit one obtains that $a(0, 0, 0)$ assumes its tree-level value,

$$a(0, 0, 0) = 1. \quad (5.33)$$

Consequently, Eq. (5.26) becomes

$$R(0) = F(0)J_m(0), \quad (5.34)$$

whereas, in the same limit, Eq. (5.17) gives directly

$$\widehat{R}(0) = \widehat{J}_m(0). \quad (5.35)$$

It is now relatively straightforward to derive a simple relation relating $R(0)$ with $\widehat{R}(0)$. Specifically, use of Eq. (2.13) and the relation (3.13) at $q^2 = 0$, yields

$$\widehat{J}_m(0) = [1 + G(0)]^2 J_m(0) = F^{-2}(0) J_m(0), \quad (5.36)$$

so that finally

$$\frac{R(0)}{\widehat{R}(0)} = F^3(0). \quad (5.37)$$

Since $F(0) > 1$, the determination of $R(0)$ from $\widehat{R}(0)$ might be error prone; in the case studied in the previous section, at $\mu = 4.3$ GeV one has $F(0) = 2.86$, which furnishes $R(0) = 1.58$ for the initial value $\widehat{R}(0) = 0.067$. Therefore, given also the sensitivity of the effective charge to the value of $\widehat{R}(0)$, one should ideally proceed the other way round, limiting the possible values of $\widehat{R}(0)$ through an independent measurement of $R(0)$.

VI. CONCLUSIONS

In this work we have explored the possibility of determining the complete momentum evolution of the QCD effective charge from a special kinematic limit of the three-gluon vertex corresponding to three background gluons. Given that within the BFM quantization scheme the (background) gauge invariance is preserved, the aforementioned vertex satisfies linear WIs, with no reference to the ghost sector; within the PT the same property emerges naturally, after the systematic rearrangement of an appropriate observable, following the standard pinching rules. Consequently, and in contradistinction to what happens in the case of the conventional three-gluon vertex, the longitudinal form factors of this PT-BFM vertex may be expressed *exclusively* in terms of the background gluon wave function \widehat{J}_m . By virtue of the dynamically generated gluon mass, this latter quantity, as well as the physical effective charge defined from it, are infrared finite and free of any divergences related to the perturbative Landau pole.

Particularly interesting in this context is the possibility of simulating the (Landau gauge) PT-BFM vertex on the lattice. To that end, after briefly reviewing the general theoretical feasibility of such a task, we have focused on the specifics of the vertex simulation, with special emphasis on the relevant kinematic limit that projects out the desired quantity $\widehat{J}_m(q^2)$. In addition, a preliminary numerical analysis suggests that the extraction of the effective charge is relatively insensitive to the numerical uncertainties that may infest an

actual lattice simulation. On the contrary, the reconstruction of the running gluon mass turned out to be considerably more subtle; specifically, instead of being positive-definite and monotonically decreasing, the corresponding curve displays unphysical fluctuations past 1 GeV, due to the distortion of delicate numerical cancellations.

The results presented in this article are expected to contribute to the collective effort dedicated to the deeper comprehension of the nature and properties of the QCD effective charge. In fact, the possibility of probing directly the value of $\bar{\alpha}(q^2)$ at the origin, through the corresponding lattice extraction of $\widehat{J}_m(0)$, is intriguing, and may serve as testing ground for various alternative pictures. In particular, the value of $\bar{\alpha}(0)$ is directly related to the notion of the ‘‘QCD conformal window’’, appearing in studies based on the AdS/QCD correspondence [13].

It is important to emphasize that the nature of the observable \widehat{R} , coupled with the fact that we work in the Landau gauge, results in the total annihilation of the completely longitudinal pole vertex \widehat{V} , which is intimately associated with the Schwinger mechanism of gauge-boson mass generation. In that sense, the situation is completely analogous to what happens with standard observables, where all direct effects from this particular vertex vanish, due to current conservation or general on-shellness conditions. Note that the same situation applies to the case of conventional three-gluon vertex, and its associated V ; they too cancel out completely from the corresponding lattice quantity R . Therefore, any (apparently) singular behavior that may be observed in simulations of these quantities should not be interpreted as a potential consequence of the pole vertices.

A possible determination of $\widehat{J}_m(q^2)$ can provide considerable theoretical insights that extend beyond the accurate extraction of the effective charge, and could help us explore the nonperturbative behavior of additional key dynamical ingredients. In particular, the complete integral equation that govern the evolution of $\widehat{J}_m(q^2)$ depends on the fully dressed four-gluon vertex that involves one background and three quantum gluons. The available information on this vertex is very limited at the moment; the only robust result known is the WI that is satisfied when contracted with the momentum of the background gluon. It is therefore reasonable to expect that further research will be devoted in this direction. Then it is clear that independent information on $\widehat{J}_m(q^2)$ may prove valuable for determining the structure of this elusive vertex, at least in some simple kinematic limits.

In general, the lattice simulation of the PT-BFM propagator and vertices would offer the

unique opportunity to verify explicitly powerful formal relations, connecting basic Green's function of the theory. Note, for instance, that the simulation of $\widehat{\Delta}(q^2)$ could furnish a direct confirmation of the fundamental BQI of Eq. (2.9), given that both $\Delta(q^2)$ and $G(q^2)$ have already been simulated on the lattice. In addition, the result of Eq. (5.37) may be of certain usefulness for future lattice endeavors. Specifically, one may use combinations of lattice results to probe the veracity of the (few) theoretical assumptions entering in its derivation; conversely, one may assume the validity of Eq. (5.37) and use it to validate the lattice implementation of the BFM algorithm. To be sure, such comparisons must be carried out between lattice simulations possessing similar parameters (*e.g.*, bare couplings, spacings, volumes).

Finally, note that the present considerations may be extended to include other fundamental vertices of the PT-BFM formalism, such as the vertex connecting a background gluon and a ghost-anti-ghost pair, usually denoted by $\widehat{\Gamma}_\mu$. This vertex has a rather reduced tensorial structure, and satisfies a simple Abelian WI, relating its divergence to the difference of two inverse ghost propagators. A preliminary study reveals that relations similar to (4.15) may be also obtained for the ghost dressing function. Hence, lattice simulation of $\widehat{\Gamma}_\mu$ may provide nontrivial cross-checks on the infrared behavior of this latter quantity. We hope to present the full details of the related analysis in the near future.

Acknowledgments

The research of D. I. and J. P. is supported by the Spanish MEYC under Grant No. FPA2011-23596.

-
- [1] J. M. Cornwall, Phys. Rev. **D26**, 1453 (1982).
 - [2] A. Cucchieri and T. Mendes (2007), arXiv:0710.0412 [hep-lat].
 - [3] I. Bogolubsky, E. Ilgenfritz, M. Muller-Preussker, and A. Sternbeck, Phys.Lett. **B676**, 69 (2009).
 - [4] A. Aguilar, D. Binosi, and J. Papavassiliou, PoS **LC2008**, 050 (2008).
 - [5] A. Aguilar, D. Binosi, J. Papavassiliou, and J. Rodriguez-Quintero, Phys.Rev. **D80**, 085018 (2009).

- [6] A. Aguilar, D. Binosi, and J. Papavassiliou, JHEP **1007**, 002 (2010).
- [7] Y. L. Dokshitzer, G. Marchesini, and B. R. Webber, Nucl. Phys. **B469**, 93 (1996).
- [8] L. von Smekal, R. Alkofer, and A. Hauck, Phys. Rev. Lett. **79**, 3591 (1997).
- [9] D. V. Shirkov and I. L. Solovtsov, Phys. Rev. Lett. **79**, 1209 (1997).
- [10] A. C. Aguilar, A. A. Natale, and P. S. Rodrigues da Silva, Phys. Rev. Lett. **90**, 152001 (2003).
- [11] G. M. Prosperini, M. Raciti, and C. Simolo, Prog. Part. Nucl. Phys. **58**, 387 (2007).
- [12] C. S. Fischer, J. Phys. **G32**, R253 (2006).
- [13] S. J. Brodsky, G. F. de Teramond, and A. Deur, Phys.Rev. **D81**, 096010 (2010).
- [14] A. Courtoy and S. Liuti (2013).
- [15] J. M. Cornwall and J. Papavassiliou, Phys. Rev. **D40**, 3474 (1989).
- [16] A. Pilaftsis, Nucl. Phys. **B487**, 467 (1997).
- [17] D. Binosi and J. Papavassiliou, Phys. Rev. **D66**, 111901(R) (2002).
- [18] D. Binosi and J. Papavassiliou, J.Phys.G **G30**, 203 (2004).
- [19] D. Binosi and J. Papavassiliou, Phys.Rept. **479**, 1 (2009), 245 pages, 92 figures.
- [20] L. F. Abbott, Nucl. Phys. **B185**, 189 (1981).
- [21] A. C. Aguilar and J. Papavassiliou, JHEP **12**, 012 (2006).
- [22] D. Binosi and J. Papavassiliou, Phys.Rev. **D77**, 061702 (2008).
- [23] D. Binosi and J. Papavassiliou, JHEP **0811**, 063 (2008).
- [24] P. A. Grassi, T. Hurth, and M. Steinhauser, Annals Phys. **288**, 197 (2001).
- [25] D. Binosi and J. Papavassiliou, Phys.Rev. **D66**, 025024 (2002).
- [26] P. A. Grassi, T. Hurth, and A. Quadri, Phys. Rev. **D70**, 105014 (2004).
- [27] A. Aguilar, D. Binosi, and J. Papavassiliou, JHEP **0911**, 066 (2009).
- [28] A. C. Aguilar and J. Papavassiliou, Phys.Rev. **D81**, 034003 (2010).
- [29] A. Aguilar, D. Binosi, and J. Papavassiliou, Phys.Rev. **D84**, 085026 (2011).
- [30] D. Binosi, D. Ibanez, and J. Papavassiliou, Phys.Rev. **D86**, 085033 (2012).
- [31] M. Binger and S. J. Brodsky, Phys. Rev. **D74**, 054016 (2006).
- [32] D. Binosi and A. Quadri, Phys.Rev. **D85**, 121702 (2012).
- [33] A. Cucchieri and T. Mendes, Phys.Rev. **D86**, 071503 (2012).
- [34] W. J. Marciano and H. Pagels, Phys. Rept. **36**, 137 (1978).
- [35] J. S. Ball and T.-W. Chiu, Phys. Rev. **D22**, 2550 (1980).
- [36] A. Cucchieri, A. Maas, and T. Mendes, Phys.Rev. **D74**, 014503 (2006).

- [37] P. Pascual and R. Tarrach, Lect. Notes Phys. **194**, 1 (1984).
- [38] A. I. Davydychev, P. Osland, and O. V. Tarasov, Phys. Rev. **D54**, 4087 (1996).
- [39] N. Ahmadiniazi and C. Schubert, Nucl.Phys. **B869**, 417 (2013).
- [40] J. M. Cornwall (2012), 1211.2019.
- [41] R. Jackiw and K. Johnson, Phys. Rev. **D8**, 2386 (1973).
- [42] R. Jackiw, In *Erice 1973, Proceedings, Laws Of Hadronic Matter*, New York 1975, 225-251 and M I T Cambridge - COO-3069-190 (73,REC.AUG 74) 23p (1973).
- [43] J. M. Cornwall and R. E. Norton, Phys. Rev. **D8**, 3338 (1973).
- [44] E. Eichten and F. Feinberg, Phys. Rev. **D10**, 3254 (1974).
- [45] E. C. Poggio, E. Tomboulis, and S. H. H. Tye, Phys. Rev. **D11**, 2839 (1975).
- [46] J. S. Schwinger, Phys. Rev. **125**, 397 (1962).
- [47] J. S. Schwinger, Phys. Rev. **128**, 2425 (1962).
- [48] M. Luscher and P. Weisz, Nucl.Phys. **B452**, 213 (1995).
- [49] R. F. Dashen and D. J. Gross, Phys. Rev. **D23**, 2340 (1981).
- [50] H. Neuberger, Phys.Lett. **B183**, 337 (1987).
- [51] L. F. Abbott, Acta Phys. Polon. **B13**, 33 (1982).
- [52] L. Giusti, M. Paciello, C. Parrinello, S. Petrarca, and B. Taglienti, Int.J.Mod.Phys. **A16**, 3487 (2001).
- [53] J. C. Taylor, Nucl. Phys. **B33**, 436 (1971).